

Fabrication and Characterization of Bubble-driven Micromixers

Matthew David Rolleston

Rochester Institute of Technology, 1 Lomb Memorial Drive, Rochester, NY;

Abstract—Microfluidics differ from conventional fluid flows in that viscous forces dominate. As a result, microfluidics offer unprecedented control over fluid flows. The precise manipulation of fluids can be applied anywhere from healthcare in medical diagnostics to pharmaceutical companies miniaturizing reactions to reduce reagent consumption. In order to apply microfluidics as a comprehensive solution, unit operations must be performed such as mixing, sorting and dilution. This work investigates the fabrication and characterization of bubble-driven micromixers using inertial micropump technology. Unlike macroscopic fluid flows with turbulence, transport phenomena become restricted in microfluidics. Active mixing approaches apply external forces (such as thermal or electric) to enhance mixing. A pulse sent to the fabricated microheater will form a vapor bubble. As this vapor bubble collapses, the disruption in the fluids cause mixing. The micromixer design was verified to mix fluids using particle tracking software. Still images of the bubble formation and collapse were obtained by using a stroboscopic laser effect.

Index Terms—MEMS, Microheaters, Microfluidics, Mixing

I. INTRODUCTION

MICROFLUIDICS applications are becoming more commonplace in industries such as healthcare, where lab-on-chip technology is being used for medical diagnostics. Pharmaceutical companies are using microfluidic principles to miniaturize reactions, reducing reagent consumption. A challenge that is faced when working with microfluidic devices is mixing operations [1]. As channel diameters become smaller and the Reynolds number is decreased, laminar flow becomes apparent. The nature of laminar flows is to flow without disruption, therefore other techniques must be employed to mix flows. Using a surface MEMS process, a microheater was fabricated to explore the ability to mix laminar flows via metastable boiling. This active approach to mixing would provide a low cost, area efficient alternative to passive mixing techniques.

II. THEORY

Inertial micropump technology can be used to displace fluids within a microchannel. The micropump consists of a microheater device that can cause mechanical actuation of a fluid by forming a vapor bubble when the fluid is heated. The vapor bubble has a rapid growth and decay during which fluid will be displaced. Locating the microheater near the walls of the microchannels will allow for control of which direction the fluid will pump [1]. Similarly, this same principle can be used to mix two fluids within the microchannel. A microheater positioned on the laminar boundary between two fluids, once

pulsed, should cause enough disruption in the fluid to mix them. Fig. 1 illustrates the testing setup. Two fluids will be flowed into a microchannel, where a Reynolds number of 30 will be targeted. One inlet port will be seeded with particles in DI water, while the other just DI water. Once the microheater is pulsed, the outlet ports will be examined to see the ratio of particles across the two legs.

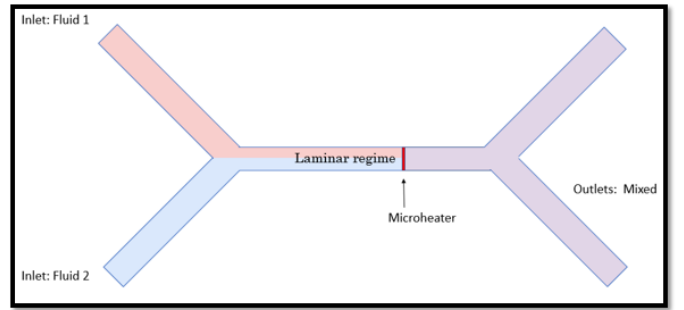


Fig. 1. Illustration of microheater mixing laminar flow.

To estimate the heat response for the proposed microheaters with its given stack, a 1D Fourier's Law for heat transfer model was used to estimate the thermal resistance beneath the polysilicon heater [2]:

$$R_{\theta} = \frac{x}{A \cdot k} \quad (1)$$

where:

R_{θ} = thermal resistance of the SiO_2 ($^{\circ}\text{C}/\text{W}$)

x = length of the thermal path (m)

A = cross-sectional area of the polysilicon heater (m^2)

k = thermal conductivity of SiO_2 ($1.4\text{W}/\text{m}^{\circ}\text{C}$)

Assuming there is no power loss, the voltage needed to heat the polysilicon to a given temperature is represented as:

$$V_{app} = \sqrt{\frac{\Delta T \cdot R}{R_{\theta}}} \quad (2)$$

where:

ΔT = temperature change of the polysilicon heater ($^{\circ}\text{C}$)

R = resistance of the polysilicon heater (Ω)

These equations were utilized to choose specific material thicknesses and device dimensions to allow for an operating voltage under 100V.

III. FABRICATION

Using a surface MEMS process, microheaters were fabricated on silicon substrates.

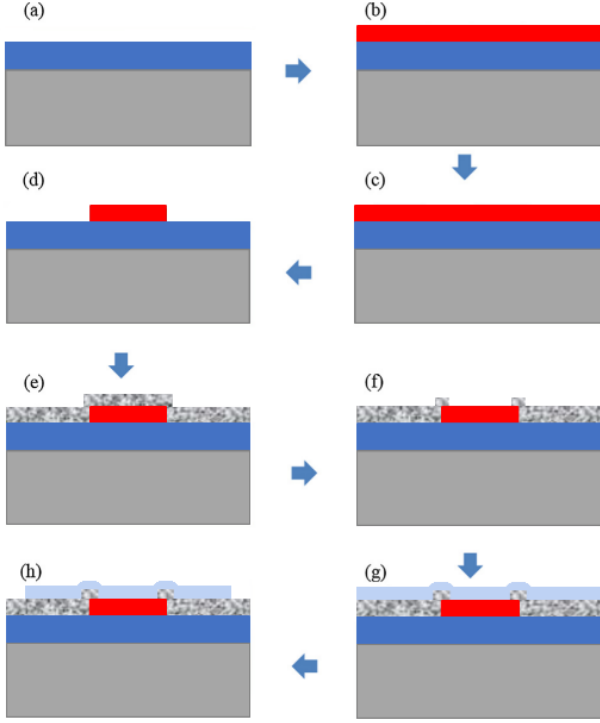


Fig. 2. Microheater process flow. Color code: silicon (gray), silicon dioxide (blue), polysilicon (red), aluminum (marble), thin silicon dioxide layer (light blue).

The fabrication process is illustrated in Fig. 1. Since these devices were fabricated on silicon, which has a higher thermal conductivity than desired, first $5\mu\text{m}$ of SiO_2 is deposited via tetraethyl orthosilicate (TEOS) chemical vapor deposition (CVD). This will act as a thermally resistive buffer layer between the silicon substrate and the microheater device (Fig. 1a). A $1\mu\text{m}$ thick layer of polysilicon is then deposited via low pressure chemical vapor deposition (LPCVD) (Fig. 1b). The polysilicon is then subsequently doped with a dose of $2\text{E}16$ of P31 at 70KeV by ion implantation and annealed at 1050°C . The targeted sheet resistance of the doped polysilicon was $20\Omega/\text{sq}$ (Fig. 1c). Level 1 lithography was done to define the polysilicon. Device dimensions were targeted to have a length of $300\mu\text{m}$ and width of $200\mu\text{m}$ (Fig. 1d). To make contact to the polysilicon, $1\mu\text{m}$ of aluminum was DC sputtered (Fig. 1e). Level 2 lithography was done to define the aluminum (Fig. 1f). In order to protect the device from the fluids that may come into contact with it, an electrically isolating layer of roughly 70nm of SiO_2 was deposited (Fig. 1g). The SiO_2 over the contact pads was then etched in a buffered oxide etch to allow for electrical contact to be made to the devices (Fig. 1h).

IV. RESULTS AND DISCUSSION

A. Temperature Calibration

Temperature calibration was done by placing the microheater devices in an oven. Resistance values were recorded

at certain temperature readings. This allows for a thermal coefficient of resistance (TCR) to be backed out for the polysilicon. For these devices the polysilicon had a positive TCR of $6.61\text{E-}4\text{ }1/^\circ\text{C}$ (Fig. 3).

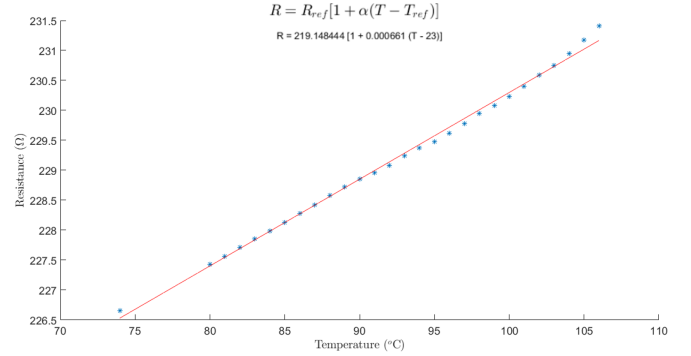


Fig. 3. Resistance measurements as a function of temperature.

With the TCR of the polysilicon, the temperature of the microheater can be modeled. Fig. 4 shows the 1D heat transfer model vs. the TCR extrapolation for predicting the microheater's temperature for a given power. This proves that in this case, a 1D heat transfer model is sufficient in modeling the temperature response for a given stack on a silicon substrate.

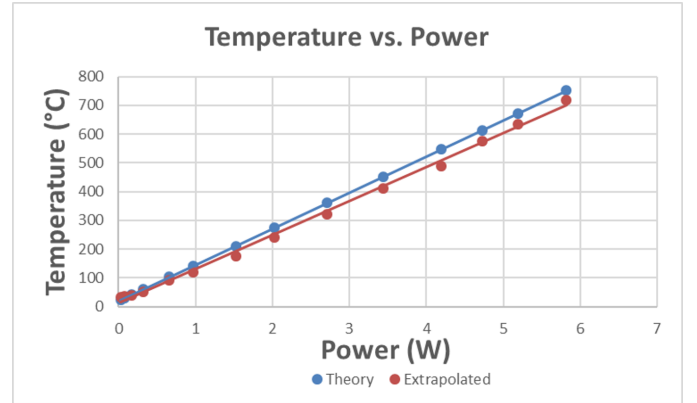


Fig. 4. 1D heat transfer model vs. thermal coefficient of resistance extrapolation.

It is important to note that these two models are for a DC case. During mixing experiments a transient signal is sent to the microheaters. It is believed that the fire conditions of the microheater are around 300°C as this would be the boiling regime where metastable boiling is seen.

B. Mixing Verification

To verify that the microheaters can be used to mix fluids, first a steady state laminar flow was established in DI water. To visualize laminar flow the bottom inlet leg was seeded with $7\mu\text{m}$ particles. This allows for particle tracking to be utilized to create flow streamlines and better visualize the mixing response.

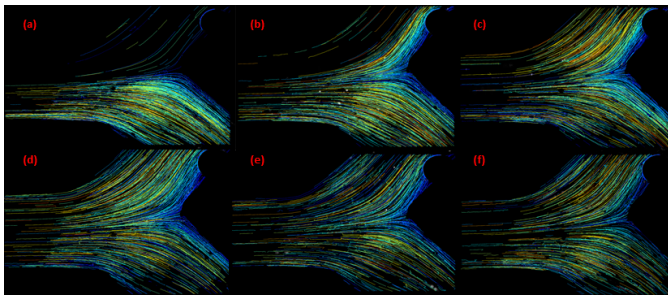


Fig. 5. Metastable Boiling Frequency Streamlines – displays particle streamlines across the entire video for various firing frequencies at 65V with $10\mu s$ pulse. (a) 0 Hz, (b) 5 Hz, (c) 10 Hz, (d) 15 Hz, (e) 20 Hz, and (f) 25 Hz.

Fig. 5 shows the response of firing the microheater with a $10\mu s$, 65V pulse at increasing frequencies. It is shown that for a given flow rate, as the frequency of which the microheater is fired, the more mixing will occur. At a flow rate of .01ml/min, a 65V $10\mu s$ pulse at 15Hz is shown to fully mix the two fluids.

C. Bubble Nucleation

To verify that the mixing mechanism of these devices is bubble-driven, a stroboscopic laser was used to capture still images of the formation of collapse of the bubble.

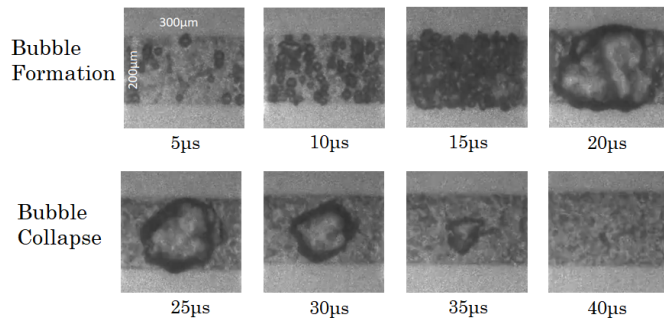


Fig. 6. Metastable boiling at 65V with $10\mu s$ pulse.

Fig. 6 shows the bubble formation and collapse after an initial pulse of 65V for $10\mu s$ the bubble is shown to grow to nearly the same size as the microheater, roughly $10\mu s$ after the initial pulse. This is because there is thermal lag in the system and once the microheater surface is heated, this heat must be transferred to the water above and allow for it to change states. The bubble is seen to collapse in around $20\mu s$.

V. CONCLUSIONS

A surface MEMS microheater was designed and fabricated. Using the same principles as an inertial micropump, the fabricated microheaters were shown to actively mix laminar flows in microchannels due to the formation and collapse of a drive bubble.

VI. FUTURE WORK

Future designs could utilize flow sensors to measure flow rates within the microchannels and create a feedback loop to control firing frequency. This would ensure that even with a changing flow rate, mixing will always be optimized.

APPENDIX

- | | |
|----------------------------------|-----------------------------------|
| 1. Starting Wafer | 13. ET55 - Metal Etch |
| 2. CL01 - RCA Clean | 14. ET07 - Resist Strip |
| 3. OX07 – Deposit $5\mu m$ TEOS | 15. OX04 – Al Sinter |
| 4. CV01 – LPCVD Poly $1\mu m$ | 16. CV03 - TEOS - 700\AA |
| 5. SD01 – Spin on Dopant | 17. PH03 - Level 3 Contact Cut |
| 6. OX04 – Anneal | 18. ET06 - TEOS Etch |
| 7. PH03 – Level 1 Poly | |
| 8. ET08 – Poly Etch | |
| 9. ET07 - Resist Strip | |
| 10. CL01 - RCA Clean, HF Dip | |
| 11. ME01 - Metal Deposition - Al | |
| 12. PH03 - level 2 Metal | |

Fig. 7. Microheater Process Flow

ACKNOWLEDGMENTS

This project was supported in part by HP Inc. Thank you to Dr. Lynn Fuller of Rochester Institute of Technology for advisement. Fabrication support was provided by the SMFL staff.

REFERENCES

- [1] E. D. Tornaiainen, A. N. Govyadinov, D. P. Markel, and P. E. Kornilovitch, "Bubble-driven inertial micropump," *Physics of Fluids*, vol. 24, p. 18, Dec 2012.
- [2] Fraden, J. (2016). *Handbook of Modern Sensors*. Cham: Springer International Publishing.
- [3] B. Hayes, A. Hayes, A. Ferreira, J. Krisher, M. Rolleston, 2018. "Pulsatory Mixing of Laminar Flow using Inertial Micro-Pumps". Unpublished.